PCCP

The reaction of C_2H radicals with C_2H_6: Absolute rate coefficient measurements for $T = 295$–800 K, and quantum chemical study of the molecular mechanism

B. Ceursters, H. M. T. Nguyen, M. T. Nguyen, J. Peeters and L. Vereecken*

Department of Chemistry, University of Leuven, Celestijnenlaan 200F, B-3001 Leuven, Belgium. E-mail: Luc.Vereecken@chem.kuleuven.ac.be

Received 17th April 2001, Accepted 31st May 2001
First published as an Advance Article on the web 29th June 2001

The absolute rate coefficient of the title reaction was measured for the first time at elevated temperatures, using a pulsed laser photolysis/chemiluminescence (PLP/CL) technique. C_2H radicals were generated by excimer laser photodissociation of acetylene at 193 nm, and pseudo-first-order decays of thermalised C_2H were monitored in real-time using the $CH(A\,^2\Delta \rightarrow X\,^2\Pi)$ chemiluminescence from the reaction of C_2H with excess O_2 as an ethynyl probe. The rate coefficients, measured over the temperature range 295–779 K, exhibit a slight non-Arrhenius behaviour and can be represented by $k_{C_2H+C_2H_6}(T) = 1.19 \times 10^{-12}\ T^{0.54\pm0.20} \exp[(180 \pm 70)\ K/T]$ cm^3 molecule^{-1} s^{-1}. *Ab initio* calculations were performed at the MP2 and CCSD(T) levels of theory to elucidate the molecular mechanism of the C_2H + alkane reactions. It is concluded that direct H-abstraction, leading to C_2H_2 + alkyl radical, has by far the lowest energy barrier, $\approx$3 kJ mol^{-1}, whereas substitution and insertion reactions face barriers in excess of 100 kJ mol^{-1} and are therefore not competitive.

1. Introduction

The ethynyl radical C_2H is a key intermediate in a wide variety of distinctive environments, both natural and man-made, such as hydrocarbon combustion where it may be involved in soot formation,[1] interstellar chemistry[2] and planetary atmospheres.[3] To understand fully the importance of the C_2H radical in these drastically different environments, the rates of reaction of C_2H with a wide range of compounds must be characterised over very broad temperature ranges. The rate constants of the reaction of C_2H with species such as alkanes, C_2H_2, H_2O, H_2 and NO have been measured over wider temperature ranges, showing fast reactions with low or even negative Arrhenius activation energies.[4–14] In this paper, we present direct experimental determinations of the rate coefficient of the $C_2H + C_2H_6$ reaction over the temperature range 295–779 K, using a pulsed laser photolysis/chemiluminescence (PLP/CL) technique, combined with theoretical quantum chemical calculations on the molecular mechanism of the reaction. This work is part of a wider study of the temperature dependences of the rates of C_2H reactions, and the development of a structure–activity relationship for C_2H + alkane reactions, in which $C_2H + C_2H_6$ serves as a model reaction. Several measurements of $k_{C_2H+C_2H_6}$ at room temperature have been reported, most of them relative. Tarr *et al.*[15] and Cullis *et al.*[16] measured the rate constant at 300 K of the $C_2H + C_2H_6$ reaction relative to that of $C_2H + C_2HBr$; using $k_{C_2H+C_2HBr} = 1.7 \times 10^{-10}$ cm^3 molecule^{-1} s^{-1},[17] the data of Tarr *et al.* yield $k_{C_2H+C_2H_6} = 6.68 \times 10^{-11}$ cm^3 molecule^{-1} s^{-1}, while those of Cullis *et al.* result in $k_{C_2H+C_2H_6} = (9.02 \pm 0.67) \times 10^{-11}$ cm^3 molecule^{-1} s^{-1}. Laufer[18] obtained $k_{C_2H+C_2H_6} = (6.5 \pm 0.4) \times 10^{-12}$ cm^3 molecule^{-1} s^{-1} from the time-dependence of the C_2H_2 reaction product. Okabe[19,20] measured the rate constant of the title reaction relative to that of $C_2H + C_2H_2$; using the presently accepted, nearly temperature-independent value for the reference rate constant,[5,7,13,14] $k_{C_2H+C_2H_6} = (1.4 \pm 0.2) \times 10^{-10}$ cm^3 molecule^{-1} s^{-1}, Okabe's data result in $k_{C_2H+C_2H_6} = (3.4 \pm 0.5) \times 10^{-11}$ cm^3 molecule^{-1} s^{-1}. Lander *et al.*[21] reported an absolute, direct measurement of $k_{C_2H+C_2H_6} = (3.6 \pm 0.2) \times 10^{-11}$ cm^3 molecule^{-1} s^{-1} at room temperature.

The only temperature-dependent determination of $k_{C_2H+C_2H_6}$ thus far is the absolute measurement performed by Opansky and Leone[10] over the T-range 150–359 K; they reported an Arrhenius expression with a very slight negative T-dependence: $k_{C_2H+C_2H_6}(T) = (3.5 \pm 0.3) \times 10^{-11} \exp[(2.9 \pm 16)K/T]$ cm^3 molecule^{-1} s^{-1}, which corresponds to $k_{C_2H+C_2H_6}(298\ K) = (3.5 \pm 0.5) \times 10^{-11}$ cm^3 molecule^{-1} s^{-1}.

The formation of an alkyl radical and acetylene by direct H-abstraction is generally thought to be an important if not major channel of alkane + ethynyl reactions. However, to our knowledge no quantitative product data are available. The low $k_{C_2H+C_2H_6}$ value derived by Laufer[18] from the $[C_2H_2]$ growth profile (see above) may even suggest that H-abstraction is only a minor channel. In two papers on C_2H + alkane reactions, Opansky and Leone[9,10] argue that H and/or CH_3 substitution by the C_2H radical might be important product channels in these reactions.

From the above, it is clear that (i) rate coefficient data are needed at elevated temperatures, over an as wide as possible range, for reliable extrapolation to flame conditions, and (ii) the nature of the reaction products and the molecular mechanism of the reaction must be established. In this paper, we address both these issues.

2. Experimental technique

The absolute rate coefficient $k_{C_2H+C_2H_6}$ was measured using a pulsed laser photolysis/chemiluminescence (PLP/CL) set-up that has been described earlier, and that was validated and employed by this group in the study of several other C_2H reactions.[4–6,13,22,23] Basically, ethynyl radicals were generated pulse-wise by C_2H_2 photolysis, and their pseudo-first-order decay was monitored in real-time by measuring the 430

 DOI: 10.1039/b103415b

nm CH* chemiluminescence resulting from its reaction with O_2, present in constant (excess) concentration. A gas flow, consisting of C_2H_2, O_2, C_2H_6 and He as carrier gas, was continuously fed through a resistively heatable Al_2O_3 tube with internal SiO_2 coating into a stainless-steel photolysis cell. An excimer laser beam traverses the cell *via* baffled side-arms equipped with Suprasil windows and crosses the internal ceramic tube at right angles through two 15 mm diameter holes. Optical emissions from the irradiated reaction volume are monitored through a Suprasil window facing the Al_2O_3 tube mouth. The temperature in the irradiated, probed volume is measured by a coaxially movable, calibrated chromel/alumel thermocouple. The total pressure in the photolysis cell is measured by a Datametrics Barocel Type 600 sensor; in most of the experiments, the pressure was 10 Torr, with He as bath gas. All gases were obtained commercially; the purities were: He 99.9990% (Air Liquide), C_2H_2 99.5% (Hoek Loos), O_2 99.995% (Air Liquide) and C_2H_6 10.4% in He 99.9990% (UCAR). The acetone in the commercial acetylene was removed by a trap cooled by a dry ice–acetone mixture. The flow rates of the gases were regulated and measured by calibrated mass flow controllers and the concentrations of the individual reactants were determined from their fractional flows and from the total pressure. The total gas flow was sufficiently large to refresh the gas in the observed volume between successive laser shots. Photodissociation of C_2H_2 to generate C_2H was achieved at 193 nm using an ArF excimer laser (EMG 101 MSC, Lambda Physik; 30 mJ per pulse at 10 Hz; pulse length $\approx$20 ns); the beam section was telescoped down to 8 × 3 mm. In the experimental conditions, quenching of electronically and/or vibrationally excited C_2H radicals possibly generated in the photolysis of acetylene is sufficiently fast to ensure that only ground state C_2H reactions are monitored at $t \geqslant 5$ μs.[13,22] To suppress production of C_2 and CH by multiphoton processes, the laser fluence was kept below 120 mJ cm^{-2}. The progress of the reaction (t = 5–20 μs) is monitored by detection of the time-resolved 430 nm CH($A\,^2\Delta \rightarrow X\,^2\Pi$) chemiluminescence (CL) from electronically excited CH($A\,^2\Delta$) produced by the reaction of C_2H with molecular oxygen, present in a large and constant concentration.[13,23] The 430 nm CH* chemiluminescence from the reaction volume was collected by suitable optics, and focused onto a photomultiplier through a narrow-bandpass interference filter (centred at 430 nm). The photomultiplier output was fed to an SRS Type 250 boxcar-integrator. The delay between the laser firing and the opening of the boxcar gate was gradually increased by 0.1 μs every tenth laser pulse, while the gate width was kept constant at 1 μs. Ethynyl decays were analysed over reaction times of ~3–20 μs. Ethane, O_2 and C_2H_2 were each always present in a very large excess over C_2H (initial concentration $\approx 10^{12}$ cm^{-3}), ensuring also that contributions from secondary and/or radical–radical reactions to the C_2H decay are negligible. Transport of C_2H out of the observed volume by diffusion or convection (time scale of ms in the experimental conditions) cannot compete with its chemical reaction losses (time scale of μs).

3. Experimental results

Fig. 1 shows a typical pseudo-first-order decay and semilog plot of the relative C_2H concentration *vs.* reaction time. The decay of C_2H can be expressed by:

$$[C_2H]_t = [C_2H]_0 \exp(-k't)$$

with

$$k' = k_{C_2H+C_2H_6}[C_2H_6] + k_{C_2H+C_2H_2}[C_2H_2] + k_{C_2H+O_2}[O_2]$$

The bimolecular rate coefficients $k_{C_2H+C_2H_6}$ were determined by measuring the decay constant k' at varying $[C_2H_6]$ (0–5×10^{15} cm^{-3}), and at fixed C_2H_2 and O_2 concentrations of

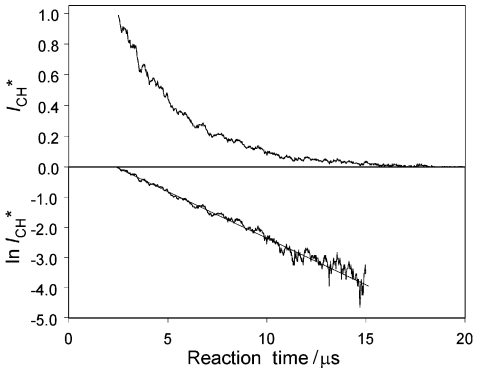

Fig. 1 Typical pseudo-first-order decay and semilog plot of the relative C_2H concentration *vs.* reaction time, at T = 584 K, P_{tot} = 10 Torr, $[O_2] = 4.95 \times 10^{15}$ molecules cm^{-3}, $[C_2H_2] = 4.92 \times 10^{14}$ molecules cm^{-3}; $[C_2H_6] = 2.09 \times 10^{15}$ molecules cm^{-3}. The straight line represents a weighted linear least-squares fit.

$\approx 5 \times 10^{14}$ and $\approx 5 \times 10^{15}$ cm^{-3}, respectively. The slope of the linear plot of k' *vs.* $[C_2H_6]$ yields the rate coefficient $k_{C_2H+CH_2H_6}$, whereas the ordinate intercept is equal to the contributions of acetylene and oxygen to the total decay constant: $k_{C_2H+C_2H_2}[C_2H_2] + k_{C_2H+O_2}[O_2]$. A typical k' *vs.* $[C_2H_6]$ plot is shown in Fig. 2 for T = 584 K; about 15–20 k' measurements were made at varying C_2H_6 concentrations in the range 0–5×10^{15} cm^{-3} for each temperature. The value of the ordinate intercept at all temperatures agrees perfectly, within a few per cent, with the expected value of $k_{C_2H+CH_2}[C_2H_2] + k_{C_2H+O_2}[O_2]$ as derived from our separate measurements of the $k_{C_2H+C_2H_2}$ and $k_{C_2H+O_2}$ rate coefficients.[4,6,20]

The complete set of $k_{C_2H+C_2H_6}$ data in the range T = 295–800 K is given in Table 1, and shown as an Arrhenius plot in Fig. 3. The stated total errors, amounting to about 10%,

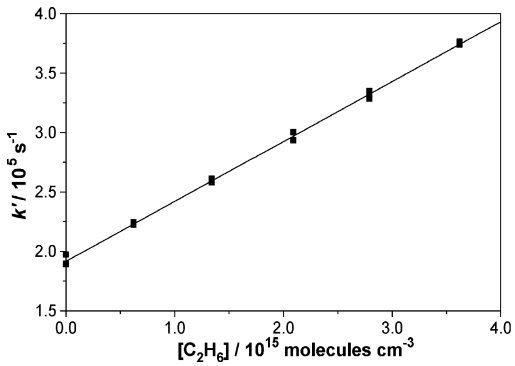

Fig. 2 Pseudo-first-order decay constants k' plotted *vs.* $[C_2H_6]$ at T = 584 K, P_{tot} = 10 Torr, $[C_2H_2] = 4.92 \times 10^{14}$ molecules cm^{-3}, $[O_2] = 4.95 \times 10^{15}$ molecules cm^{-3}. The solid line represents a weighted linear least-squares fit to the data points.

Table 1 Bimolecular rate coefficients $k_{C_2H+C_2H_6}$ for the reaction of $C_2H + C_2H_6$

T/K	1000/T (K^{-1})	$k_{C_2H+C_2H_6}$/cm^3 molecule^{-1} s^{-1}
295	3.39	$(4.68 \pm 0.47) \times 10^{-11}$
327	3.06	$(4.87 \pm 0.49) \times 10^{-11}$
351	2.85	$(4.81 \pm 0.48) \times 10^{-11}$
387	2.58	$(4.76 \pm 0.48) \times 10^{-11}$
415	2.41	$(4.83 \pm 0.48) \times 10^{-11}$
450	2.22	$(4.77 \pm 0.48) \times 10^{-11}$
511	1.96	$(5.11 \pm 0.51) \times 10^{-11}$
584	1.71	$(5.00 \pm 0.50) \times 10^{-11}$
668	1.50	$(5.16 \pm 0.52) \times 10^{-11}$
729	1.37	$(5.51 \pm 0.55) \times 10^{-11}$
779	1.28	$(5.56 \pm 0.56) \times 10^{-11}$

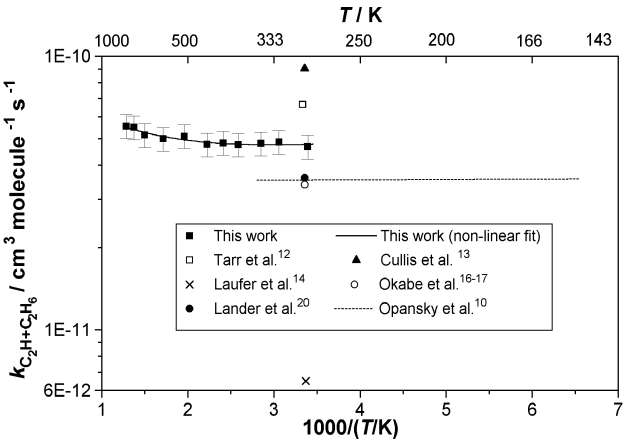

Fig. 3 Arrhenius plot showing the rate coefficient $k_{C_2H+C_2H_6}$ obtained for the gas-phase reaction of $C_2H + C_2H_6$. The full curve represents the modified Arrhenius expression $k_{C_2H+C_2H_6}(T) = 1.19 \times 10^{-12} T^{0.54\pm0.20}$ exp[(180 ± 70) K/T] cm^3 molecule^{-1} s^{-1}. Errors bars include possible systematic errors.

include estimated maximum systematic errors due to inaccuracies in the absolute reactant concentrations and in other experimental parameters; the actual variances based on repeated, independent measurements separated in time by many months, are of the order of 5%. The Arrhenius plot shows an upward curvature; the non-Arrhenius behaviour can be expressed by a three-parameter modified Arrhenius equation derived by non-linear least-squares analysis:

$$k_{C_2H+C_2H_6}(T) = 1.19 \times 10^{-12} T^{0.54\pm0.20} \times \exp[(180 \pm 70)\ \mathrm{K}/T]\ \mathrm{cm}^3\ \mathrm{molecule}^{-1}\ \mathrm{s}^{-1}$$

4. Quantum chemical calculations

The mechanism of the C_2H + alkane reactions, of which $C_2H + C_2H_6$ is a model reaction, can proceed by three different mechanisms: (a) direct H-abstraction, (b) substitution of an alkyl group or H-atom by C_2H and (c) insertion of C_2H in a C–C or C–H bond. The H-abstraction reaction will only lead to C_2H_2 + an alkyl radical, while the other two mechanisms can lead to a much wider variety of products. In order to determine which of these three mechanisms is most favourable, we characterised the relevant part of the potential energy surface (PES) of the $C_2H + C_2H_6$ reaction. Since it was not our intention here to explore fully the [C_4H_7] PES, but rather to determine which molecular mechanism(s) are important in the C_2H + alkane reactions, we focused on the characterisation of the entrance transition states and subsequent reaction products.

All calculations were performed using the GAUSSIAN98 suite of programs.[24] Geometry optimizations and harmonic vibrational wavenumber calculations were conducted using molecular orbital theory at the Hartree–Fock level of theory, and second-order perturbation theory, MP2/6-31G*. The MP2 zero-point vibration energies (ZPE) were scaled down by a uniform factor of 0.95. Based on the MP2 geometries, single point electronic energies were also calculated at the MP2/6-311++G** and MP2/6-311++G(3df,2p) levels of theory, as well as with coupled-cluster theory, with single, double, and perturbative corrections for triple excitations, CCSD(T)/6-311++G**. In the MP2 and CCSD(T) calculations, the core electrons were kept frozen. For the open-shell systems the unrestricted formalism [UHF, UMP2, UCCSD(T)] was used.

Fig. 4 shows selected geometric parameters for the most relevant minima and transition states, while the calculated absolute and ZPE-corrected relative energies are listed in Table 2. The zero-point vibrational energy for C_2H at the MP2/6-31G** level of theory, 46.2 kJ mol^{-1}, is severely overestimated. This is mainly due to an incorrect description of the degenerate C_2H bending vibration with a vibrational wavenumber of 831.6 cm^1, compared with the experimental value of 371 cm^{-1},[25] and due to a rather high spin contamination of

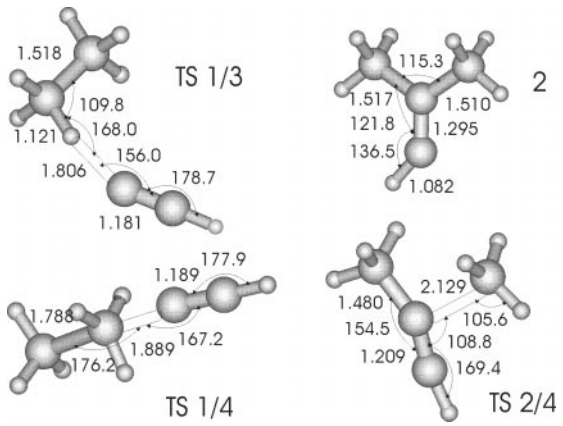

Fig. 4 Selected optimized geometrical parameters for intermediates and transition states in the $C_2H + C_2H_6$ reaction. Bond lengths are given in angstroms and bond angles in degrees.

Table 2 Calculated total energies (hartree) and ZPE-corrected relative energies (kJ mol^{-1}) for relevant points on the $C_2H + C_2H_6$ potential energy surface

	Total energy					ZPE	Relative energy
Structure	MP2 6-31G**	MP2[a] 6-311++G**	MP2[a] 6-311++G(3df,2p)	CCSD(T)[a] 6-311++G**	CCSD(T) (est.)[b] 6-311++G(3df,2p)	MP2 6-31G**	CCSD(T) 6-311++G(3df,2p)
C_2H	−75.350 76	−76.379 91	−76.419 22	−76.423 84	−76.463 15	40[c]	
C_2H_6	−79.543 40	−79.571 67	−79.620 31	−79.616 54	−79.665 18	203.4	
C_2H_2	−77.081 67	−77.113 30	−77.156 88	−77.141 25	−77.184 83	68.6	
C_2H_5	−78.875 89	−78.904 79	−78.950 90	−78.948 49	−78.994 60	162.1	
CH_3	−39.692 71	−39.708 66	−39.731 40	−39.733 64	−39.756 38	80.6	
C_3H_4	−116.273 00	−116.316 83	−116.384 88	−116.361 89	−116.429 94	147.3	
$C_2H + C_2H_6$ (**1**)	−155.894 16	−155.951 58	−156.039 53	−156.040 38	−156.128 33	243.5	0
$C_2H_2 + C_2H_5$ (**3**)	−155.957 56	−156.018 09	−156.107 78	−156.089 74	−156.179 43	230.7	−146
$CH_3 + C_3H_4$ (**4**)	−155.965 71	−156.025 49	−156.116 28	−156.095 53	−156.186 32	227.9	−167
$(CH_3)_2CC-H$ (**2**)	−156.001 00	−156.057 46	−156.149 00	−156.136 82	−156.228 33	259.3	−248
TS 1/3	−155.891 35	−155.950 48	−156.040 10	−156.038 47	−156.128 09	245.5	+3
TS 1/4	−155.847 12	−155.911 56	−156.004 27	−155.995 95	−156.088 66	247.1	+108
TS 2/4	−155.930 98	−155.992 40	−156.084 27	−156.076 35	−156.168 22	246.3	−102
TS 1/2							~ +220[d]

[a] Single point calculations on the MP2/6-31G** geometries. [b] Estimated as CCSD(T)/6-311++G** + [MP2/6-311++G(3df,2p) − MP2/6-311++G**]. [c] Adapted (see text). [d] Relative energy estimation based on HF/3-21G** calculations.

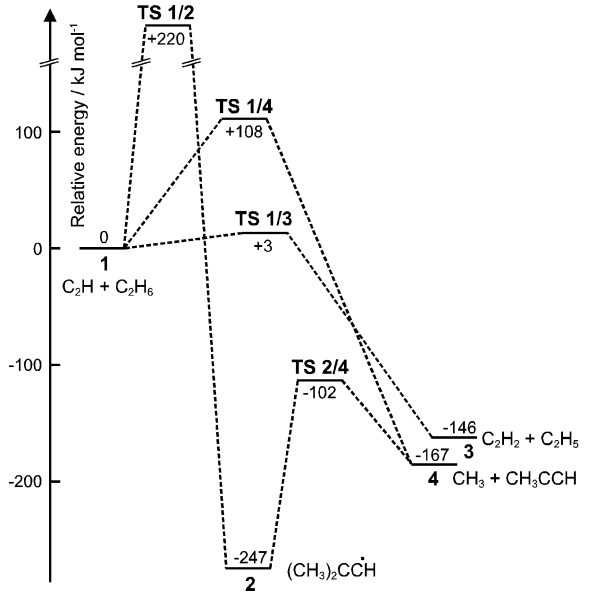

Fig. 5 Schematic potential energy profiles illustrating the different pathways of the $C_2H + C_2H_6$ reaction. Relative energies are estimated at the CCSD(T)/6-311++G(3df,2p) level of theory (see Table 2), except for **TS 1/2** which is at the HF/3-21G** level of theory.

$\langle S^2 \rangle = 1.07$ for the UHF wavefunction. Because of these MP2-specific problems, the ZPE energy for C_2H was corrected down to 40 kcal mol^{-1}, based on the results of a high-level frequency analysis at the CCSD(T)/6-311++G(2df,2p) level of theory, which performed much better in reproducing the experimentally observed wavenumbers (*e.g.* 377.6 cm^{-1} for the bending vibration). Table 2 also shows approximate values for the energies at the CCSD(T)/6-311++G(3df,2p) level of theory, estimated by adding the difference between the MP2/6-311++G** and MP2/6-311++(3df,2p) energies to the CCSD(T)/6-311++G** energy, in the assumption that the basis set effect is nearly identical at the MP2 and CCSD(T) levels.

Fig. 5 shows the relevant section of the potential energy surface. The transition state for direct hydrogen abstraction, **TS 1/3**, lies only 3 kJ mol^{-1} above the energy level of the reactants. Given this low energy barrier and the exothermicity of this reaction, 146 kJ mol^{-1}, the transition state is an early, reactant-like transition state in which the forming C–H bond is still 1.8 Å long, with the breaking C–H bond at 1.12 Å. The transition state for CH_3/C_2H substitution, proceeding through the S_N2-like nucleophilic substitution transition state **TS 1/4**, is located at 108 kJ mol^{-1} above the separated reactants. The similar transition state for H/C_2H substitution is expected to lie even higher, considering the higher steric hindrance at the transition state, and the much stronger C–H bond that needs to be broken. In the $C_2H + CH_4$ reaction, the analogous H/C_2H substitution transition state is located at 72 kJ mol^{-1} above the reactants.[5] The third possible reaction channel, C_2H insertion in the C–C bond in ethane, would lead to the stable 2-methyl-1-propen-1-yl radical, adduct **2**, at -248 kJ mol^{-1} below the reactants, which can, amongst others, dissociate to $CH_3 + CH_3CCH$ through **TS 2/4**. We were able to characterise the corresponding insertion transition state **TS 1/2** only at the HF/3-21G** level of theory, with a very high relative energy of 220 kJ mol^{-1} above the reactants. The transition state for insertion in a C–H bond is expected to be even higher in energy due to the stronger C–H bond, and the less favourable H-orbital properties. Despite extensive efforts to find an insertion transition state at a higher level of theory, our calculations always converged to lower-lying transition states not related to the insertion channel.

5. Discussion

The rate coefficient at room temperature measured in this work, $k_{C_2H+C_2H_6}(300\ K) = 4.7 \times 10^{11}$, is in the range 3.5×10^{-11}–9×10^{-11} cm^3 $molecule^{-1}$ s^{-1} laid out by earlier measurements.[10,15,16,21] Similar to the experimental results of Opansky and Leone for the $T = 150$–359 range,[10] we find an almost negligible T-dependence up to 450 K, though our results show a slight upward curvature for $T > 450$ K. It should be noted that the two earlier absolute k (300 K) determinations,[10,21] which are both a factor of 1.3 lower than the result obtained in this work, pertain to the observed decay of C_2H radicals in the (0,0,0) vibrational ground state, whereas the result of this work represents the decay of the (weighted) sum of C_2H vibration states contributing to the CH* chemiluminescence by reaction with O_2. Thus, a higher reactivity of the bending-vibration excited state (370 cm^{-1}, doubly degenerate), combined with slight departure from the thermal equilibrium vibration populations in either of the experiments, might explain the small differences in the absolute k values and in their temperature dependence.

The large differences in the relative energies of the **TS 1/3**, **TS 1/4** and **TS 1/2** transition states as calculated in this work unequivocally lead to the conclusion that the $C_2H + C_2H_6$ reaction will proceed by direct hydrogen abstraction, while substitution and insertion reactions occur only at negligibly slow rates, even at the highest flame temperatures. This finding agrees with an earlier *ab initio* study by our group on the $C_2H + CH_4$ reaction,[5] which concluded that direct H-abstraction leading to $C_2H_2 + CH_3$ is by far the most favourable channel.

The rate coefficient data measured in this work can be represented by the modified Arrhenius expression: $k_{C_2H+C_2H_6}(T) = 1.19 \times 10^{-12}\ T^{0.54\pm0.20} \exp[(180 \pm 70)\ K/T]$ cm^3 $molecule^{-1}$ s^{-1}. The power of the T^n function, $n \approx 0.5$, is much smaller than the value of 2–2.5 usually found for this type of H-abstraction process, including the reaction of ethynyl with H_2[22] and CH_4.[5] This is entirely consistent with a variational transition state expected for a reaction with a very low energy barrier (VTST theory).[26,27] At increasing temperatures, the variational transition state geometry will gradually shift along the reaction coordinate towards tighter, more product-like structures, resulting in rate coefficients that increasingly depart from the too high values predicted by conventional TST theory. This will result in a smaller than usual curvature of the Arrhenius plot. A behaviour of this type was predicted by Zhang *et al.*[28] for the $C_2H + H_2$ reaction, which has an energy barrier of about 10 kJ mol^{-1}, for temperatures higher than $\approx$800 K. It is not surprising that for the $C_2H + C_2H_6$ reaction, which has a much lower barrier, such variational behaviour is already apparent at more moderate temperatures.

No attempts were made in this work to predict the rate coefficients by VTST theory. One of the reasons is the probable error of at least 5 kJ mol^{-1} on the calculated barrier height, due in part to uncertainties on the zero point vibrational energies derived from MP2 frequencies (see above). An energy error of this magnitude entails a rate coefficient error at room temperature of almost an order of magnitude. Theoretical rate constant predictions for this reaction would therefore require energy and frequency calculations at much higher levels of theory, in order to obtain accuracies matching those of the experimental rate coefficient data.

6. Conclusion

In this study, the absolute rate coefficients of the gas-phase reaction of the ethynyl radical with ethane, $C_2H + C_2H_6$, were measured for the first time at elevated temperatures. The result in the 295–800 K range can be expressed by the modi-

fied Arrhenius equation $k_{C_2H+C_2H_6}(T) = 1.19 \times 10^{-12}$ $T^{0.54\pm0.20}$ exp[(180 ± 70) K/T] cm^3 molecule^{-1} s^{-1}. High-level *ab initio* calculations revealed that the direct H-abstraction reaction channel, leading to $C_2H_2 + C_2H_5$, is by far the most favourable reaction path. These calculations, combined with the earlier calculations on $C_2H + CH_4$,[5] warrant an extension of this conclusion to the homologous series of the alkanes, which we predict to all react by direct hydrogen abstraction, leading to acetylene and an alkyl radical. Obviously, the nature of the hydrogens being abstracted, *i.e.* leading to a primary, secondary or tertiary product radical, will affect the rate coefficient and will, therefore, for more complicated (branched) alkanes, affect the product distribution. Absolute rate coefficient measurements over a wide T-range and the construction of a site-specific structure–activity relationship (SAR) for the temperature-dependent rate coefficient and product distribution for alkanes will be the subject of a later paper.

Acknowledgements

The authors are indebted to the Fund for Scientific Research Flanders (FWO-Vlaanderen) and the KULeuven Research Council (BOF Fund) for continuing support.

References

1 R. D. Kern and K. Xie, *Prog. Energy Combust. Sci.*, 1991, **17**, 191.
2 W. M. Jackson, Y. Bao and R. S. Urdahl, *J. Geophys. Res.*, 1991, **96**, 17569.
3 G. R. Gladstone, M. Allen and Y. L. Yung, *Icarus*, 1996, **119**, 1.
4 B. Ceursters, PhD Thesis, KULeuven, 2000.
5 B. Ceursters, H. M. T. Nguyen, J. Peeters and M. T. Nguyen, *Chem. Phys. Lett.*, 2000, **329**, 412, and references cited therein.
6 B. Ceursters, H. M. T. Nguyen, J. Peeters and M. T. Nguyen, *Chem. Phys.*, 2000, **262**, 243, and references cited therein.
7 J. O. P. Pedersen, B. J. Opansky and S. R. Leone, *J. Phys. Chem.*, 1993, **97**, 6822.
8 B. J. Opansky, P. W. Seakins, J. O. P. Pedersen and S. R. Leone, *J. Phys. Chem.*, 1993, **97**, 8583.
9 B. J. Opansky and S. R. Leone, *J. Phys. Chem.*, 1996, **100**, 4888.
10 B. J. Opansky and S. R. Leone, *J. Phys. Chem.*, 1996, **100**, 19904.
11 R. J. Hoobler, B. J. Opansky and S. R. Leone, *J. Phys. Chem. A*, 1997, **101**, 1338.
12 T. Kruse and P. Roth, *J. Phys. Chem. A*, 1997, **101**, 2138.
13 H. Van Look and J. Peeters, *J. Phys. Chem.*, 1995, **99**, 16284, and references cited therein.
14 M. Koshi, N. Nishida and H. Matsui, *J. Phys. Chem.*, 1995, **96**, 5875.
15 A. M. Tarr, O. P. Strausz and H. E. Gunning, *Trans. Faraday Soc.*, 1965, **61**, 1946.
16 C. F. Cullis, D. J. Hucknall and J. V. Shepherd, *Proc. R. Soc. London, Ser. A*, 1973, **335**, 525.
17 H. Brachhold, U. Alkemade and K. H. Homann, *Ber. Bunsen-Ges. Phys. Chem.*, 1988, **92**, 916.
18 A. H. Laufer, *J. Phys. Chem.*, 1981, **85**, 3828.
19 H. Okabe, *Can. J. Chem.*, 1983, **61**, 850.
20 H. Okabe, *J. Chem. Phys.*, 1983, **78**, 1312.
21 D. R. Lander, K. G. Unfried, G. P. Glass and R. R. Curl, *J. Phys. Chem.*, 1990, **94**, 7759.
22 J. Peeters, H. Van Look and B. Ceursters, *J. Phys. Chem.*, 1996, **100**, 15124, and references cited therein.
23 K. Devriendt, H. Van Look, B. Ceursters and J. Peeters, *Phys. Chem. Lett.*, 1996, **261**, 450.
24 GAUSSIAN98, Revision A.5, M. J. Frisch, G. W. Trucks, H. B. Schlegel, G. E. Scuseria, M. A. Robb, J. R. Cheeseman, V. G. Zakrzewski, J. A. Montgomery Jr., R. E. Stratmann, J. C. Burant, S. Dapprich, J. M. Millam, A. D. Daniels, K. N. Kudin, M. C. Strain, O. Farkas, J. Tomasi, V. Barone, M. Cossi, R. Cammi, B. Mennucci, C. Pomelli, C. Adamo, S. Clifford, J. Ochterski, G. A. Petersson, P. Y. Ayala, Q. Cui, K. Morokuma, D. K. Malick, A. D. Rabuck, K. Raghavachari, J. B. Foresman, J. Cioslowski, J. V. Ortiz, B. B. Stefanov, G. Liu, A. Liashenko, P. Piskorz, I. Komaromi, R. Gomperts, R. L. Martin, D. J. Fox, T. Keith, M. A. Al-Laham, C. Y. Peng, A. Nanayakkara, C. Gonzalez, M. Challacombe, P. M. W. Gill, B. Johnson, W. Chen, M. W. Wong, J. L. Andres, C. Gonzalez, M. Head-Gordon, E. S. Replogle and J. A. Pople, Gaussian, Pittsburgh, PA, 1998.
25 H. Kanamori and E. Hirota, *J. Chem. Phys.*, 1988, **89**, 3962.
26 D. M. Wardlaw and R. A. Marcus, *Chem. Phys. Lett.*, 1984, **110**, 230.
27 D. M. Wardlaw and R. A. Marcus, *J. Chem. Phys.*, 1985, **83**, 3462.
28 X. Zhang, Y. Ding, Z. Li, X. Huang and C. Sun, *J. Phys. Chem. A*, 2000, **104**, 8357.